JOURNAL OF VIROLOGY, May 1996, p. 2720–2729 Vol. 70, No. 5
0022-538X/96/$04.00+0

The UCUAAAC Promoter Motif Is Not Required for High-Frequency Leader Recombination in Bovine Coronavirus Defective Interfering RNA

RUEY-YI CHANG,† RAJESH KRISHNAN,‡ AND DAVID A. BRIAN*

Department of Microbiology, University of Tennessee, Knoxville, Tennessee 37996-0845

Received 2 October 1995/Accepted 23 January 1996

The 65-nucleotide leader on the cloned bovine coronavirus defective interfering (DI) RNA, when marked by mutations, has been shown to rapidly convert to the wild-type leader of the helper virus following DI RNA transfection into helper virus-infected cells. A model of leader-primed transcription in which free leader supplied in *trans* by the helper virus interacts by way of its flanking 5′UCUAAAC3′ sequence element with the 3′-proximal 3′AGAUUUG5′ promoter on the DI RNA minus strand to prime RNA replication has been used to explain this phenomenon. To test this model, the UCUAAAC element which occurs only once in the BCV 5′ untranslated region was either deleted or completely substituted in input DI RNA template, and evidence of leader conversion was sought. In both cases, leader conversion occurred rapidly, indicating that this element is not required on input RNA for the conversion event. Substitution mutations mapped the crossover region to a 24-nucleotide segment that begins within the UCUAAAC sequence and extends downstream. Although structure probing of the bovine coronavirus 5′ untranslated region indicated that the UCUAAAC element is in the loop of a prominent stem and thus theoretically available for base pair-directed priming, no evidence of an unattached leader early in infection that might have served as a primer for transcription was found by RNase protection studies. These results together suggest that leader conversion on the DI RNA 5′ terminus is not guided by the UCUAAAC element and might arise instead from a high-frequency, region-specific, homologous recombination event perhaps during minus-strand synthesis rather than by leader priming during plus-strand synthesis.

A major unresolved question regarding coronavirus transcription is how the genomic 5′-terminally encoded leader becomes fused onto each of the 3′-coterminal subgenomic mRNAs. One proposed scheme, the leader priming hypothesis, states that a free leader with its 3′ flanking consensus sequence of 5′UCUAAAC3′, a consensus among mammalian coronaviruses, recognizes its complementary promoter at intergenic sites on the genomic minus strand to prime transcription by the polymerase extension of a trimmed 3′ leader terminus (1, 2, 21, 32, 43). In an experimental transcription system which uses a synthetic mouse hepatitis virus (MHV) defective interfering (DI) RNA genome, the UCUAAAC motif, presumably as its complement on the genomic minus strand, has been demonstrated to function as the minimal promoter for synthesis of subgenomic mRNA (17, 27).

The leader priming mechanism has also been used to explain a high-frequency leader recombination event on the coronavirus DI RNA genome during its replication (21, 30). The phenomenon was first described in MHV as leader switching in which it was observed that the 5′-terminal leader in the cloned MHV JHM-derived DI RNA acquires the leader of the MHV A59 helper virus after transfection of DI RNA into helper virus-infected cells (30). From these experiments, it was envisioned that perhaps there was a leader priming of DI RNA replication (16, 21, 30). That is, the promoter 3′AGAUUUG5′ sequence near the DI RNA minus-strand 3′ terminus (near the antileader) directs leader-primed replication in a manner possibly identical to leader-primed transcription. In the case of MHV DI RNA, leader switching is known to require a 9-nucleotide (nt) sequence, UUUAUAAAC, mapping immediately downstream of the leader-flanking UCUAAAC element on DI RNA (16, 30). The mechanistic basis for this requirement has not been described (see Discussion). We have observed the leader recombination phenomenon in bovine coronavirus (BCV) DI RNA as a leader reversion event (7). In these experiments, a cloned BCV DI RNA with engineered internal leader mutations was found upon transfection to lose the introduced mutations, if it replicated, and to acquire the leader sequence of the helper virus. 5′-terminal truncations of up to 8 nt were not lethal, but truncations of 13 nt or greater prevented replication and presumably, therefore, acquisition of the wild-type leader (7).

Here we have used the BCV DI RNA replication system to examine the role of the consensus leader-flanking UCUAAAC sequence in the leader conversion event. BCV DI RNA provides an advantage over MHV in this analysis by possessing a single UCUAA sequence element, part of the UCUAAAC motif, in its 210-nt 5′ genomic untranslated region (UTR) (7, 10). The UCUAAAC sequence motif maps at nt 64 through 70 and thus forms part of the downstream flank of the leader. In MHV, on the other hand, UCUAA sequence repeat elements occur two times in MHV A59 and three to four times in MHV JHM (21, 40). These are postulated optional fusion sites for MHV subgenomic transcription initiation (1, 23, 29, 31, 39, 40, 46, 47). Only single fusion sites have been observed in BCV subgenomic transcription (10), possibly because of the singular UCUAAAC element, thus making BCV an attractive system

* Corresponding author. Phone: (423) 974-4030. Fax: (423) 974-4007. Electronic mail address: BRIAN@utkvx.utk.edu.

† Present address: Institute of Biochemistry, National Yang-Ming University, Taipei, Taiwan.

‡ Present address: NIAID Laboratory of Molecular Microbiology, National Institutes of Health, Bethesda, MD 20892.

with which to analyze the mechanistic details of the UCUA AAC sequence element in the fusion process.

In this study, we have learned by structure probing that the BCV 5′-proximal leader-associated UCUAAAC element is probably in the loop of stem II of a cloverleaf-like structure and is thus theoretically available for directing a base-paired priming event were it to occur. Through mutational analysis, we sought to determine the role of the UCUAAAC and its flanking sequence in the leader reversion event. Since the helper virus in our experimental system was derived from a DI RNA-free, persistently infected cell line (12) and has mutated genomic 5′ termini (GAUUAUG and GAAUAUG rather than GAUUGUG) (11), we describe the leader repair process as leader conversion rather than leader reversion. (Thus, the terms leader switching [which could imply a two-way exchange], leader repair, leader reversion, and leader conversion have all been used to describe the high-frequency 5′-terminal leader recombination event discussed in this report.) We have learned that the UCUAAAC sequence can be deleted or completely substituted and leader conversion will still take place. To determine the site of crossover, point mutations were made throughout a 128-nt stretch downstream of the UCUAAAC sequence. A region of high-frequency crossover was determined to be within a 24-nt segment that includes the last base of the UCUAAAC sequence element and also a UUUAUA AA palindrome. These results, along with the inability to demonstrate a free (unattached) leader species, suggest to us that leader conversion may happen through a high-frequency, region-specific, homologous recombination event during minus-strand synthesis rather than by a leader-priming mechanism during plus-strand synthesis.

MATERIALS AND METHODS

Virus, cells, and cloned BCV DI RNA. A three-times plaque-purified stock of BCV Mebus strain (24) was used to establish a persistently infected cell culture (12). At 120 days, the cells producing virus were free of detectable DI RNA, and recovered virus grew to titers of 10^8 PFU/ml and had a mutated 5′ terminus (5′GAUUAUG and 5′GAAUAUG rather than 5′GAUUGUG present in the original wild-type virus stock [11]). From this, a DI RNA-free stock of virus at 1.8×10^8 PFU/ml was prepared and used as helper virus. Human rectal tumor cells (HRT-18) (24) were used in all experiments. The 2.2-kb BCV DI RNA that was cDNA cloned into pGEM3Zf(−) vector (Promega), given a reporter sequence, and named pDrep1 (Fig. 1A and B) (7) was used in the mutagenesis and replication studies. It possesses the wild-type 5′ GAUUGUG terminus. The methods used for RNA transfection and assay of DI RNA replication in transfected cells, and in cells infected with progeny virus that carry the packaged, replicated DI RNA, were as described previously (7) except that RNA was extracted from cells at 24 rather than 48 h postinfection (hpi) with progeny virus.

Enzymatic structure probing of the BCV leader. The method of Skinner et al. (42) as described by Pollack and Ganem (33) was used. For in vitro synthesis of the RNA, 5 μg of *Nco*I-linearized pDrep1 DNA (Fig. 1B) was transcribed by using 40 U of T7 RNA polymerase in a 100-μl reaction mixture. The resultant RNA was 262 nt long and contained only BCV sequence. The product was treated with RNase-free DNase (Promega), chromatographed through a Biospin 6 column (Bio-Rad), ethanol precipitated, and redissolved in 60 μl of buffer containing 70 mM *N*-2-hydroxyethylpiperazine-*N*′-2-ethanesulfonic acid (HEPES; pH 7.0), 10 mM $MgCl_2$, and 270 mM KCl. After heating at 56°C for 5 min and cooling at 37°C for 10 min, 5 μl of the RNA solution was used in a 100-μl reaction mixture containing 30 mM Tris-HCl (pH 7.5), 20 mM $MgCl_2$, 300 mM KCl, and 0.01, 0.1, or 1.0 U of RNase One (Promega) or RNase CV1 (Pharmacia). Reactions were performed on ice for 30 min and terminated by addition of 150 μl of 0.5 M sodium acetate. RNA was phenol-chloroform extracted, ethanol precipitated, redissolved, and used for primer extension with 5′-end-labeled HpaI(+) oligonucleotide (Table 1 and Fig. 1C) (34). Equal amounts of undigested RNA were used to generate a sequencing ladder with the same end-labeled oligonucleotide.

Construction of mutant DI RNAs for leader conversion analysis. Plasmid constructs were all modifications of pDrep1. Oligonucleotides used in the mutagenesis steps are described in Table 1, and restriction endonuclease sites used in making constructs are shown in Fig. 1B. pDrepM1 was generated by a PCR mutagenesis procedure in which pDrepIS1 DNA (a modified pDrep1 which carries a 27-nt intergenic promoter sequence at base 1046 [20]) and primers ISM1(−) and TGEV#8(+) were used to generate a 1,082-nt PCR product from which the 1,043-nt *Bgl*II-*Bgl*II fragment was used to replace the corresponding region in pDrepIS1. From this, the 1,091-nt *Aat*II-*Hpa*I fragment was used to replace the corresponding region in pDrep1 to form pDrepM1. pDrepM2 was similarly generated except for the use of ISM2(−) oligonucleotide in the initial mutagenesis step. pDrepM3 was generated by a PCR overlap mutagenesis procedure (7). For this, the gel-purified 791-nt PCR product from a pDrep1-templated reaction with primers GEM3Zf(−)Nde(−) and ISM3(+), the gel purified 419-nt product from a reaction with primers ISM3(−) and NdeI(+), primer GEM3Zf(−)NdeI(−), and primer NdeI(+) were used together to form a 1,183-nt PCR product from which the 1,043-nt *Bgl*II-*Bgl*II fragment was used to replace the corresponding region in pDrepIS1. From this, the 1,091-nt *Aat*II-*Hpa*I fragment was used to replace the corresponding region in pDrep1 to form pDrepM3. pS2L was generated by PCR overlap mutagenesis in which the gel-purified 438-nt PCR product from a pDrep1-templated reaction with primers S2L(−) and NdeI(+), the gel purified 927-nt product from a reaction with primers GEM3Zf(−)NdeI(−) and DM(+), primer GEM3Zf(−)NdeI(−), and primer NdeI(+) were used together to form a 1,183-nt PCR product from which the 660-nt *Nae*I-*Hpa*I fragment was used to replace the corresponding region in pDrep1. pS2R was similarly constructed except for the use of oligonucleotide S2R(−) in the first PCR mutagenesis step. p81T and p84T were generated by PCR overlap mutagenesis in which the gel-purified 409-nt PCR product from a pDrep1-templated reaction with primers 81/84(−) and NdeI(+), the gel-purified 927-nt product from a reaction with primers GEM3Zf(−)NdeI(−) and DM(+), primer GEM3Zf(−)NdeI(−), and primer NdeI(+) were used together to form a 1,183-nt PCR product from which the 660-nt *Nae*I-*Hpa*I fragment was used to replace the corresponding region in pDrep1. p81T and p84T were selected from sequenced clones. p87T and p90T were similarly constructed except for the use of oligonucleotide 87T/90T(−) in the first PCR mutagenesis step. pEM was generated by PCR overlap mutagenesis in which the gel-purified 805-nt PCR product from a pDrep1-templated reaction with primers GEM3Zf(−)NdeI(−) and EM1(+), the gel-purified 475-nt PCR product from a reaction with primers leader(−) and NdeI(+), primer GEM3Zf(−)NdeI(−), and primer NdeI(+) were used together to form a 1,183-nt PCR product from which the 660-nt *Nae*I-*Hpa*I fragment was used to replace the corresponding region in pDrep1. pSM3 was generated by PCR overlap mutagenesis in which the gel-purified 404-nt PCR product from a pDrep1-templated reaction with primers SalI(−) and BCV5′end(+), the gel-purified product 475-nt PCR product from a reaction with primers leader(−) and NdeI(+), primer leader(−), and primer BCV5′end(+) were used together to form a 593-nt PCR product from which the 108-nt *Hpa*I-*Xcm*I fragment was used to replace the corresponding region in pDrep1. The sequences of all constructs were confirmed by sequencing through the insert and junction regions.

Transfection of cells and Northern (RNA) assay for DI RNA replication. Infection of cells followed by RNA transfection with Lipofectin (Bethesda Research Laboratories), RNA blotting, and probing were performed as previously described (7) except that cells at approximately 1.5×10^6 per 35-mm-diameter dish at 50% confluency were transfected with 400 ng of RNA.

Sequencing assay on replicated DI RNA. Fifty picomoles of oligonucleotide TGEV#8b was coprecipitated in ethanol with 2.5 μg of cytoplasmic RNA, and the dried RNA was dissolved in 15 μl of water, heated for 2 min at 90°C, and cooled slowly to 42°C. This preparation was incubated for 1 h at 42°C in a 30-μl final reaction volume containing 1× reverse transcription buffer (Promega), 1 mM each deoxynucleoside triphosphate, 30 U of RNasin (Promega), and 8 U of avian myeloblastosis virus reverse transcriptase (Promega) and then heated at 75°C for 10 min. From this mixture, 2.5 μl was used for PCR amplification with oligonucleotides leader(−) and TGEV#8(+), using 25 cycles of 94°C for 1 min and 72°C for 2 min. One microliter of gel-separated PCR product was taken by punching into the electrophoretically separated band and used for asymmetric PCR sequencing as previously described (10). End-labeled oligonucleotide HpaI(+) was used as the primer for sequencing.

RNase protection assay for detection of free leader. To generate the minus-strand RNA probe, plasmid p153(−) was created by modifying pDrep1. For this, the unique *Hpa*I-*Hin*dIII fragment, which contains the entire Pol-N open reading frame and poly(A) tail (Fig. 1B), was removed, the *Hin*dIII site was made blunt with Klenow enzyme, and the plasmid was religated. The 275-nt ^{32}P-labeled riboprobe was generated with SP6 RNA polymerase after linearization of p153(−) with *Pvu*II, which cuts within the vector (Fig. 1B). The RNase protection assay was performed as previously described (7). Quantitation of RNase-protected products was done by scanning of the autoradiogram with a Bio-Rad Imaging Densitometer.

RESULTS

Structure probing of the BCV leader: evidence that the singular UCUAAAC element is in the loop of stem II in a three-stem cloverleaf-like structure. Computer analysis of the secondary structure of the BCV 5′-terminal leader and its 3′ flanking sequence (nucleotides 1 to 85) with use of the Tinoco algorithm (44) predicted two stem-loops of moderate thermodynamic stability (−8.0 and −4.4 kcal [1 cal = 4.184 J]/mol for

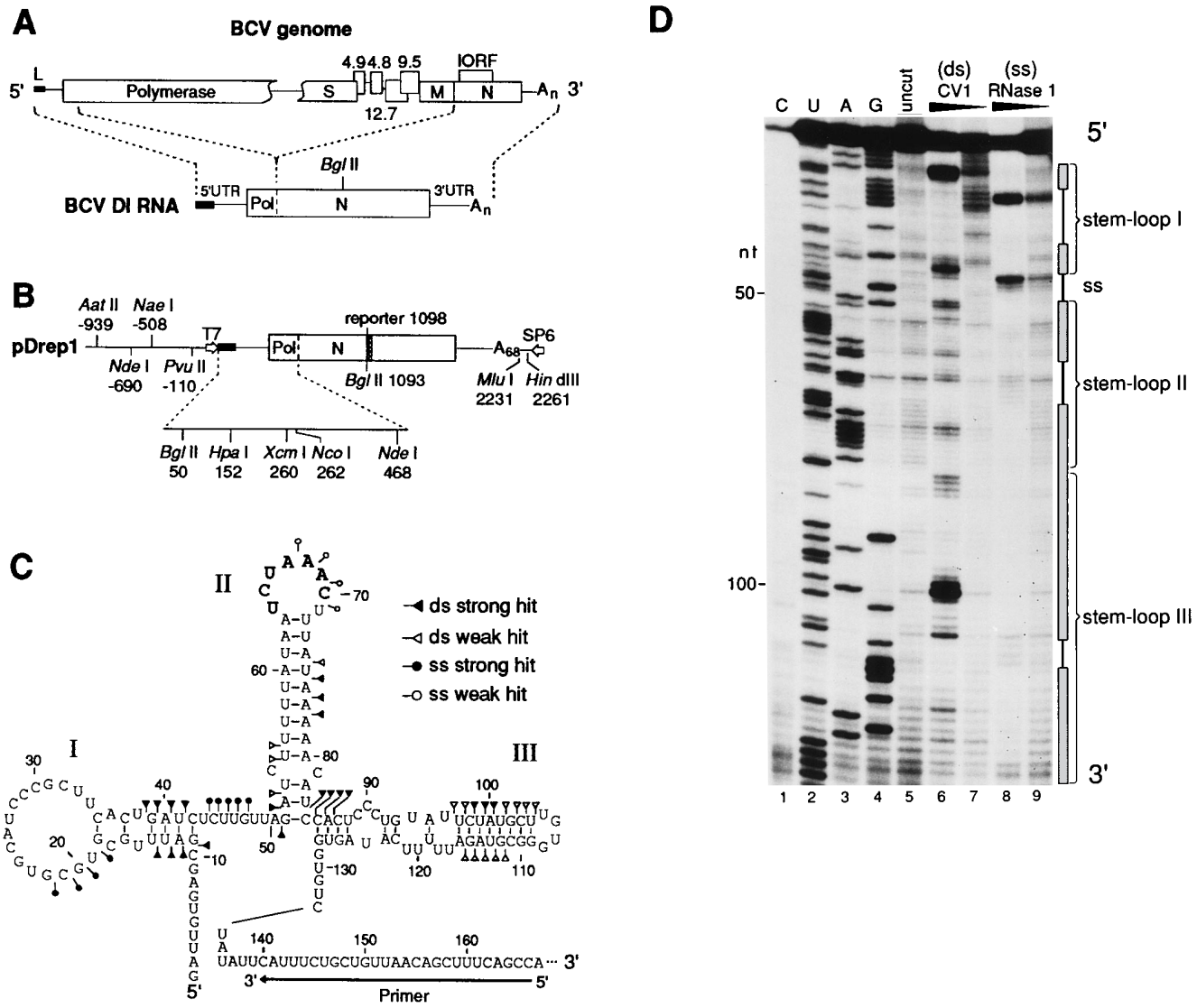

FIG. 1. Structure of the bovine coronavirus DI RNA and enzymatic structure probing of its 5′-end sequence on plus-strand RNA synthesized in vitro. (A) Structural relationship between the BCV genome and BCV DI RNA. The DI RNA is a simple fusion of the virus genomic termini. The 65-nt leader (L) is indicated by a solid rectangle. After cDNA cloning into the pGEM3Zf(−) vector, the *Bgl*II site in the DI RNA was used to insert a 30-nt in-frame reporter, creating pDrep1 (7). IORF, internal open reading frame. (B) Restriction enzyme sites in pDrep1 used for mutant construction and for generating plus-strand transcripts used for structure probing. Numbers indicate endonuclease cutting sites relative to base 1 in the pDrep1 sequence. (C) Predicted secondary structure of the BCV 5′ terminus and summary of enzymatic structure probing analysis. Stem-loops I, II, and III of the cloverleaf-like structure are identified. The UCUAAAC promoter motif is shown in boldface in the loop of stem-loop II. Sites showing strong and weak enzymatic digestion are marked. The binding region for the HpaI(+) primer (Table 1) used in the extension reaction to identify the digested products is shown. (D) A 262-nt RNA was transcribed in vitro, renatured, and cleaved with RNase specific for single-stranded (ss; RNase 1) or double-stranded (ds; CV1) regions. The positions of cleavage sites were determined by primer extension from an end-labeled primer complementary to bases 140 to 166. Lanes: 1 to 4, sequencing ladder generated from the same primer; 5, undigested RNA; 6 and 7, RNase CV1 digestion with 1.0 and 0.1 U/ml, respectively; 8 and 9, RNase 1 digested with 1.0 and 0.1 U/ml respectively. Positions of nucleotide cleavage corresponding to the respective stems and loops are indicated.

stems I and II, respectively) (7) (Fig. 1C). The UCUAAAC sequence element was found to be positioned entirely within the loop of stem-loop II. When we used the algorithm of Zuker (13) to examine other likely thermodynamic options and used a small window, two stable stem-loop possibilities appeared. The first was as shown in Fig. 1C, and the second was nearly the same except that the first 54 nt make up two small stem-loops (data not shown). In both, however, the UCUAAAC element was positioned in the loop of a stem-loop. By both the Tinoco and Zuker algorithms, a third stem-loop (−7.2 kcal/mol) designated stem-loop III could also be formed between bases 97 and 116 (Fig. 1C).

To directly test the predicted structure surrounding the UCUAAAC sequence, enzymatic probing was carried out on a positive-strand 262-nt RNA molecule representing the 5′-terminal two-thirds of the genomic 5′ UTR. For this, the RNA generated by T7 RNA polymerase on *Nco*I-linearized pDrep1 plasmid DNA (Fig. 1B) was subjected to digestion with various concentrations of RNase One (to digest single-stranded RNA) and RNase CV1 (to digest double-stranded RNA). The RNase-resistant fragments were then identified on a DNA sequencing gel after primer extension with a radiolabeled primer which binds to a region beginning 140 nt downstream of the leader (Fig. 1C). The results shown in Fig. 1D identified

TABLE 1. Oligodeoxynucleotides used in this study

Oligonucleotide[a]	Sequence (5′-3′)[b]	Binding region[c]
Leader(−)	GAGCGATTTGCGTGCGTGCATCCCGC	7–32
ISM1(−)	CTC(G/T)(A/T)GTTAGATCTTTTTATAATTTATAAAAAC	42–81
ISM2(−)	CTC(G/T)(A/T)GTTAGATCTTTTTATAACTCGGGTTTTATAAAAAC	42–81
ISM3(−)	ATCTAAACAAACATCCACTC	63–89
ISM3(+)	GAGTGGATGTTTGTTTAGATTATA	59–89
S2L(−)	CTTGTTAGATCAAAAATATTTCTAAACTTT	44–73
S2R(−)	TAATCTAAACAAATATTTTTCATCCACTCC	61–90
81/84(−)	TATAAAAA(C/T)AT(C/T)CACTCCCT	73–92
87/90(−)	AACATCCA(C/T)TC(C/T)CTGTATTC	79–98
EM1(+)	GCATAGAATTCAGGGAGTG	85–103
HpaI(+)	GGCTGAAAGCTGTTAACAGCAGAAATG	140–166
SalI(−)	CACCCATAGGTCGACAATGTCGAAG	196–219
DM(+)	GTTGATCTTCGACAATGTGACC	204–225
NdeI(+)	CCTCCAAATCATATGGACGTGTATTC	456–481
BCV5′N(+)	CTAGATTGGTCGGACTGATCGGCCCAC	573–599
TGEV#8(+)[d]	CATGGCACCATCCTTGGCAACCCAGA	1098–1123
TGEV#8b(+)	CATGGCACCATCCTTGGCA	1105–1123
GEM3Zf(−)NdeI(−)	GAGAGTGCACCATATGCGGTGT[e]	

[a] Oligonucleotide binds to either plus-sense RNA, as indicated by (+), or to minus-sense RNA, as indicated by (−).
[b] Underlined bases indicate differences from genomic sequence. Parentheses indicate that either base is present at this position in the oligonucleotide.
[c] Numbers correspond to positions in the pDrep1 plus-strand sequence.
[d] TGEV, transmissible gastroenteritis virus.
[e] Oligonucleotide GEM3Zf(−)NdeI(−) binds to vector minus-strand DNA beginning at −702 from the T7 RNA polymerase transcription start site.

seven stretches that are within helical regions and three stretches, including the UCUAAAC sequence, that make up single-stranded regions. In matching these results with structure predictions and assuming no long-range base interactions, three stem-loops forming a cloverleaf-like terminal structure that conform to the structure shown in Fig. 1C could be drawn. Except for an artifactual band at bases 65 and 66 appearing in the uncut, double-strand-specific, and single-strand-specific lanes (lanes 6 through 9), bases within the loop of stem-loop II appear weakly cut by RNase 1 (lane 8). Most of the UCUAA AC element maps within the loop of stem-loop II, therefore, and a UUUAUAAA palindromic sequence forms part of the stem of the same stem-loop.

Is this structure supported by phylogenetic evidence? Computer predictions by the Zuker algorithm have placed the UCUAAAC sequence of MHV JHM in the helical region of a stem-loop (40); however, other options from a modified Zuker program (13) place this element within a loop of other stem-loop possibilities (data not shown). To date, structure probing of the 5′ UTR of MHV or of other coronaviruses has not been reported, thus preventing a more direct comparison at this time.

The UCUAAAC element on transfected DI RNA is not required for leader conversion. Previous work had demonstrated that extensive mutations made within the BCV leader, specifically those designed to completely disrupt stem-loop I, were surprisingly not lethal for DI RNA replication following transfection into helper virus-infected cells but were instead found to yield progeny DI RNAs possessing a completely wild type leader (7). A leader priming of DI RNA replication model based on the model of leader-primed subgenomic transcription (21) would predict that the UCUAAAC motif, an internal

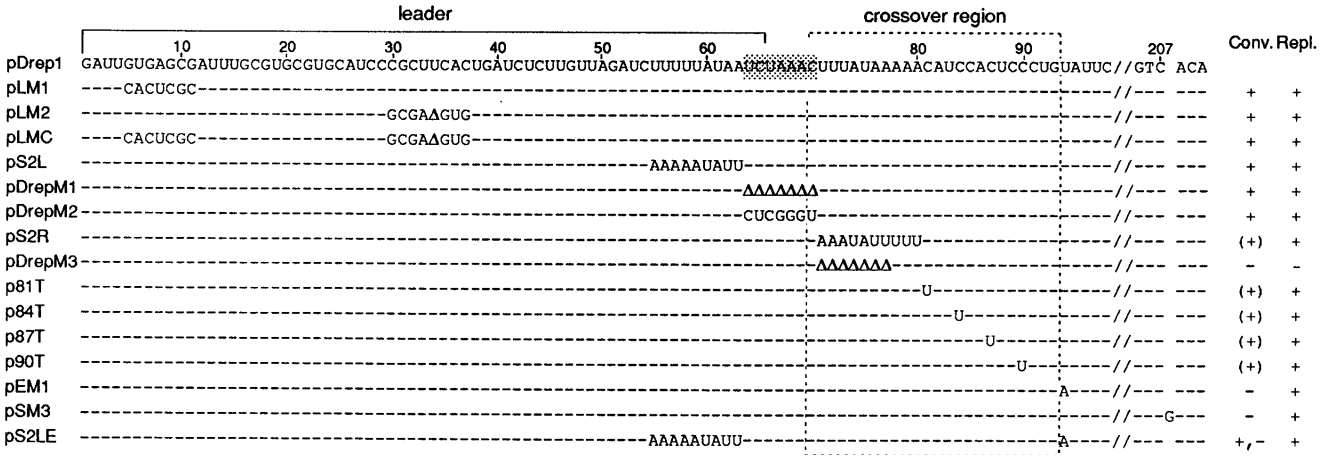

FIG. 2. Structures of mutants used in the leader conversion analyses. The 65-nt leader sequence is identified; the UCUAAAC promoter motif is shaded; the region within which crossovers occurred is shown by a box drawn with a dashed line. Δ, deleted base; (+), a mixture of mutant and wt (convertant) sequences existed in the progeny; +,−, mutations at positions 55 through 63, but not at 94, converted. Conv., conversion; Repl., replication.

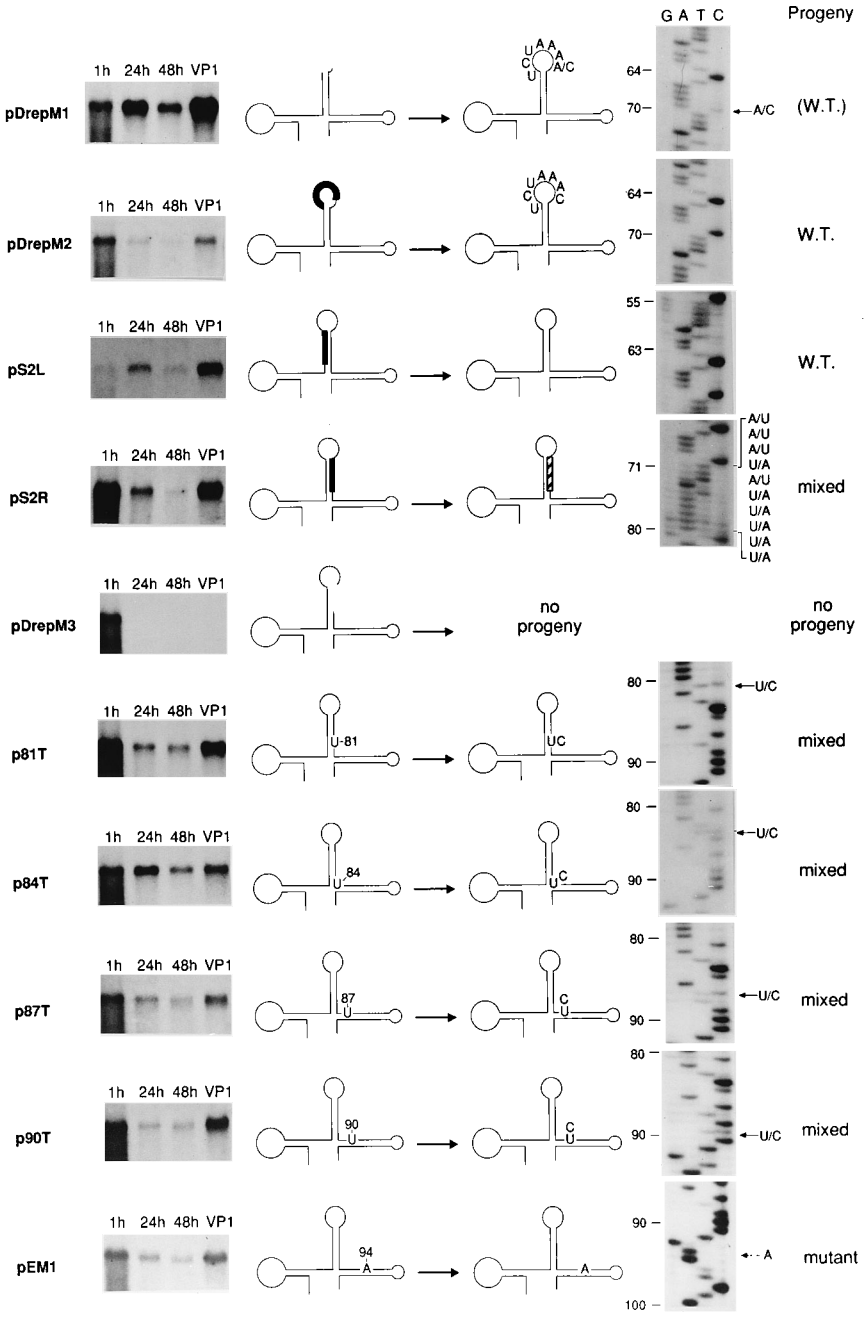

FIG. 3. Replication and conversion assays for mutants of pDrep1. Plus-strand T7 RNA polymerase-generated transcripts of the mutant plasmids linearized at the *Mlu*I site were transfected into helper virus-infected cells, and cytoplasmic RNA was extracted at the indicated times posttransfection or at 24 h after infection of cells with passage 1 progeny virus (VP1). RNA was analyzed by Northern blotting using an end-labeled probe [oligonucleotide TGEV#8(+); Table 1] that identified reporter sequence. Schematic diagrams corresponding to the cloverleaf-like structure identified in Fig. 1 summarize the mutations made and whether the mutation was converted to wild type in the first virus passage. A deleted region is indicated by a gap, a region of base substitutions is indicated by a filled box, and a region of mixed sequence is indicated by a striped box. Sequences of convertants were determined by dideoxynucleotidyl sequencing of asymmetrically amplified PCR products from RNA extracted from cells infected with VP1. Regions showing mixed sequences are identified. The progeny of pDrepM1 is described parenthetically as wild type (W.T.) and not as a mixture since, although the composition of nt 70 was mixed, the origin of A is unknown. The replication of pDrep1 transcripts was assayed in parallel in all experiments (not shown, but similar to that illustrated in reference 7).

sequence on the putative free leader of 80 to 140 nt, is an essential element in the priming mechanism. According to the model, this element would recognize its AGAUUUG complement on the DI RNA antigenome to align the primer for initiation of replication. To test this hypothesis, the leader-associated UCUAAAC sequence was deleted from pDrep1 to form pDrepM1 (Fig. 2), and evidence of DI RNA replication was sought. Figure 3 documents by Northern analysis that the transfected pDrepM1 RNA replicated and became packaged and also that the leader converted rapidly, although not with perfect fidelity. Reverse transcription-PCR sequencing of replicated molecules at virus passages 1 (shown) through 4 (not

shown) demonstrated that the convertants were approximately equal mixtures of molecules with UCUAAAC and UCUA AAA sequences. Conversion was judged to be rapid, since the progeny at 48 h and at virus passage 1, as determined by Northern analysis, was nearly as abundant as pDrep1 progeny assayed in parallel (7) (data not shown). The results with pDrepM1 transcripts were the same in three separate transfection experiments. By contrast, molecules transfected into cells in the absence of helper virus were degraded and only faintly detectable at 10 h posttransfection (6). These results indicate that the UCUAAAC motif is not required on input DI RNA for leader conversion and that an A at position 70 is tolerated for DI RNA replication in converted molecules. They further suggest that position 70 might be a crossover site in the conversion event.

To test by a second mutation whether the UCUAAAC element is needed for conversion, substitutions were made at all seven base positions to yield pDrepM2 (Fig. 2), and transcripts were tested for replication and conversion. Although accumulation at 48 h was somewhat less than for pDrep1 and pDrepM1, convertants that were completely of the wild-type UCUAAAC sequence appeared (Fig. 3), demonstrating again that the UCUAAAC sequence on input DI RNA is not required for leader conversion.

Crossover sites for leader conversion occur within a region including and immediately downstream of the UCUAAAC sequence element. The mixture of C and A at position 70 in the converted pDrepM1 (Fig. 3), the 3′-terminal position in the UCUAAAC element, suggested that this may be a crossover site between the progeny replicating molecule and the wild-type leader. To define the region of crossover, a series of substitution mutations upstream and downstream of the UC UAAAC element was tested for replication and conversion. Transcripts of mutant pS2L, created by substitutions in the nine-base sequence in the upstream leg of stem-loop II, a mutation that was also predicted to destroy the stem (Fig. 2), were rapidly repaired to wild-type sequence in replicating molecules (Fig. 3). These results demonstrated that stem II is not important in the conversion process and, along with results reported above and in reference 6 for mutants pLM1, pLM2, and pLMC (Fig. 2), suggested that the crossover point for restoration of the wild-type leader is downstream of base 69. To test this, we generated mutant pS2R, in which a 10-nt region constituting the right leg of stem II was replaced by substitutions, a change that would also disrupt the helical structure of stem II, and transcripts were tested for replication and conversion. Although the yield was somewhat less than for pDrep1 (7) or for pDrepM1 (Fig. 3), the progeny from the first virus passage was abundant and was interestingly a mixture of mostly wild-type and some mutant sequences (Fig. 3). The wild-type sequences could have arisen from at least one crossover downstream of base 78, but the mixture indicates that there are probably multiple crossover sites within the mutated region. These results also demonstrate that stem II is not required for the conversion event and that crossover may occur at one or more sites downstream of base 69.

To find the downstream limit of the crossover region, point mutations were made at base positions 81, 84, 87, 90, and 94 to form mutants p81T, p84T, p87T, p90T, and pEM1, respectively (Fig. 2), and transcripts were tested for replication and conversion. Insertions made at bases 182 (4 nt at an *Avr*II site; not shown in Fig. 2) and 208 (1 nt; mutant pSM3; Fig. 2) for other purposes were also tested. As shown in Fig. 3, all mutants containing substitutions replicated. The progeny of mutations made at 81, 84, 87, and 90, however, were mixtures of both wild-type and mutant sequences when examined at 48 h post-

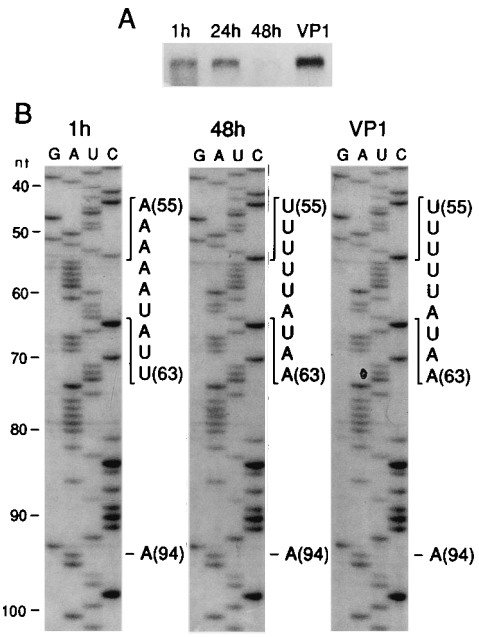

FIG. 4. Summary of replication and conversion assays for double mutant pS2LE. (A) Plus-strand T7 RNA polymerase-generated transcripts of pS2LE DNA linearized at the *Mlu*I site were transfected and assayed for replication as described for Fig. 3. (B) Sequences of DI RNA extracted at 1 and 48 h posttransfection and after 24 h following infection with passage 1 virus (VP1) were determined by dideoxynucleotidyl sequencing of asymmetrically amplified PCR products. Conversion of bases 55 through 63, but not of base 94, is noted.

transfection (not shown) and at virus passages 1 (shown) through 4 (not shown), whereas the mutation made at position 94 did not revert even after four viral passages. These results indicate that the crossover region is upstream of base 94. Mutants with insertions at positions 182 and 208, furthermore, replicated without showing evidence of conversion when tested at virus passages 1 and 4, respectively (data not shown), again indicating that crossovers downstream of base 90 were occurring extremely infrequently if at all. The region of high-frequency crossover, therefore, appears to be between nt 69 and 94.

Through a study of the double mutant pS2LE, which combined the mutations in pS2L (substitutions at bases 55 through 63) with those in pEM1 (substitution at base 94) (Fig. 2), it was demonstrated that the recombination event was not blocked by the base substitution at position 94, confirming that the high-frequency crossover was occurring upstream of this site. Although pS2LE transcripts had accumulated to a low level by 48 h posttransfection (Fig. 4A), a majority of the molecules by this time had undergone a complete conversion of bases 55 through 63 but not of base 94 (Fig. 4B). The same pattern of conversion is present at 24 hpi for passage 1 virus (Fig. 4B). Thus, the reversion patterns of all mutants taken together suggested that the region of high-frequency crossover lies between nt 69 and 94, a region that includes all of the downstream leg of stem-loop II and a small portion of loop II and stem III (Fig. 5).

The importance of the crossover region in the conversion event was emphasized by analysis of mutant pDrepM3, in which there was a 7-nt deletion made just downstream of the UCUAAAC promoter motif, a region comprising most of the 8-nt UUUAUAAA palindrome (Fig. 2). It is also homologous to part of the important 9-nt UUUAUAAAC motif found in MHV (30). Unlike deletion of the 7-nt UCUAAAC promoter motif in pDrepM1, deletion of the UUUAUAA in pDrepM3

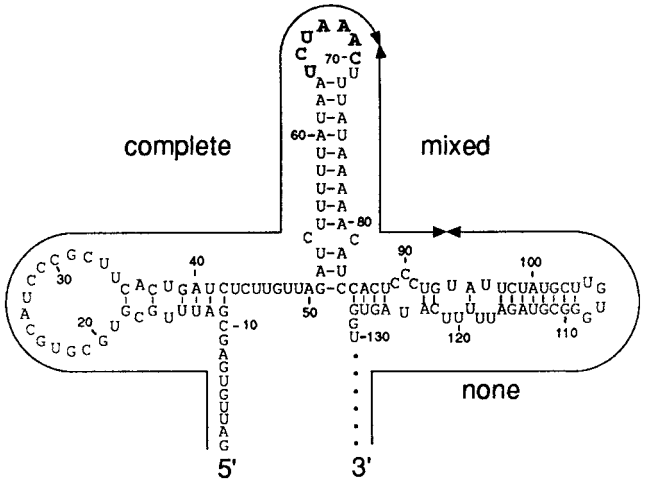

FIG. 5. Schematic summary of conversion data in relation to the proposed structure for the positive-strand leader and its flanking sequence. Regions in which mutations converted completely to wild type within one virus passage, remained mixed over a period of four virus passages, or showed no conversion over a period of four virus passages are indicated.

prevented DI RNA replication (Fig. 3). This result was obtained in three separate transfection experiments. Hence, no progeny in which the pattern of conversion could be studied were produced. This result, interestingly, contrasted with those of MHV DI RNA mutants lacking the entire 9-nt UUUAU AAAC motif. In these, there was DI RNA replication but no leader switching (16, 30).

RNase protection analysis yields no evidence of a UCUA AAC-containing free leader at early times postinfection. The leader priming of transcription hypothesis was based in part on the finding of truncated plus-strand leader-containing transcripts mostly in the size range of 80 to 140 nt in MHV-infected cells at peak times of RNA synthesis, 5 to 7 hpi (2). These were considered to function as free leaders in the priming of subgenomic transcription (2, 21, 32). To test whether similar molecules might be present in BCV-infected cells at early times after infection when the accumulation rate of subgenomic mRNAs is high and the need for leaders is great (12, 35, 38), an RNase protection experiment was done to identify potential free leader sequences between 71 and 153 nt in length. The probe used was 153 nt in length (275 nt total, including vector sequence) that would protect a 149-nt leader generated from the helper virus used in these experiments (because of the G5→A mutation in the helper virus leader [11]), and RNA samples were prepared at hourly intervals through 6 hpi and at 8 and 24 hpi. Plus-strand synthetic transcripts of pDrep1 and pNrep2 (a reporter-containing construct of N mRNA, mRNA 7 [7]) that would yield protected fragments of 153 and 75 nt, respectively, were used to ensure the reliability of the assay. As illustrated in Fig. 6, bands of these sizes were protected in the control lanes (lanes 14 and 15). In addition, we identified major protected species of 149, 71, 69, and 62 nt that became very abundant by 2 hpi (lanes 6 through 13). From the sizes of the protected fragments and of known BCV leader-mRNA junction sequences (10), it was determined that in addition to the 149-nt fragment corresponding to virus genomic RNA (mRNA 1), the 71-nt fragment corresponded to what would be protected from the N mRNA (mRNA 7). The 69-nt fragment corresponded to what would be protected from several mRNA species, including the HE mRNA (mRNA 2-1), S mRNA (mRNA 3), 4.8-kDa (4.8K) protein mRNA (mRNA 4), and

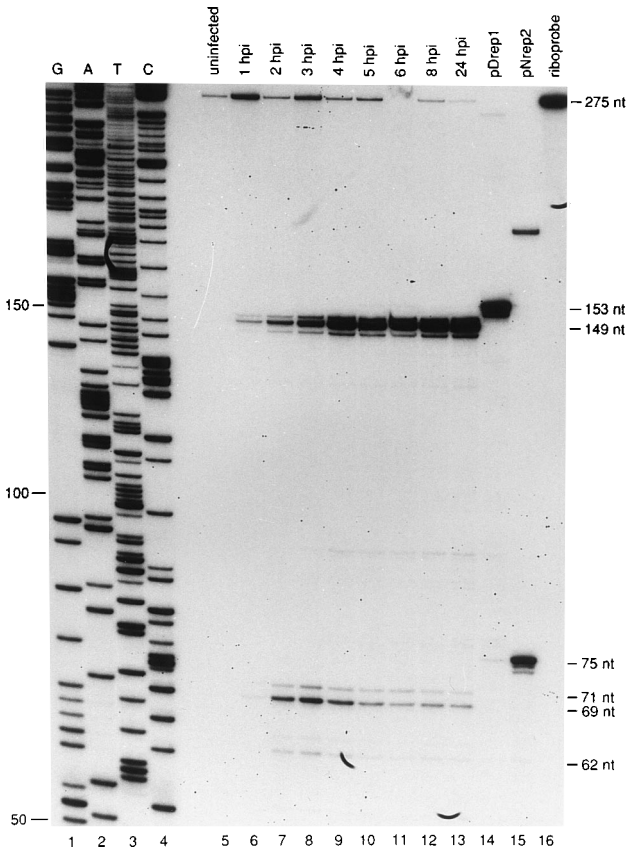

FIG. 6. RNase protection assay for free leader. Cells were infected with BCV, and cytoplasmic RNA was extracted at the times indicated. RNA was hybridized to radiolabeled minus-strand transcript that was complementary to the first 153 nt of genomic 5′ UTR (identical to the first 153 nt of pDrep1) and 122 nt of plasmid DNA and then was digested with RNase A. Precipitated products were electrophoresed on a denaturing sequencing gel of 6% polyacrylamide. Lanes: 1 to 4, sequencing ladder generated from end-labeled forward primer for pGEM3Zf(−), using p153(−) DNA as the template; 5 to 16, as indicated. pNrep2 is a cDNA clone of the BCV N mRNA carrying the 30-nt TGEV reporter sequence (7). Note that the protected transcripts for pDrep1 and pNrep2 will be 4 nt longer since they possess the 5′GAUUG sequence of the probe, whereas the virus used in this study has mutated 5′ termini of 5′GAUUA and 5′GAAUA. Thus, RNase A will cut at base position 4 in the probe.

12.7K protein mRNA (mRNA 5). The 62-nt fragment corresponded to M mRNA (mRNA 6) and the 9.5K protein mRNA (mRNA 5-1). A faint 64-nt fragment is of unknown origin but may have resulted from protection by the 35K protein mRNA (mRNA 2) for which the leader junction is not known for the Mebus strain of BCV. Note that these sizes differ from the characterized BCV leader junction lengths (10) because the RNase-susceptible pyrimidines on the minus-sense probe do not coincide with the terminal bases in the leader junctions. Free leader would be predicted to be between 71 and 149 nt in size (2) if BCV behaved the same as MHV in this regard. Only minor species of approximately 90 and 135 nt were identified as possible candidates for free leader, but these did not appear until 3 hpi, long after the time free leader would be needed for the synthesis of early mRNAs (12). These are, therefore, possibly degraded products of the genomic 5′ UTR. Thus, species of protected RNA that might have resulted from heterogeneous unattached leaders were not apparent at all between 0 and 2 hpi, and they represented less than 0.5% of total detectable protected RNA at 3 hpi and less than 6% at 8 hpi. We therefore conclude there is probably no leader in BCV-in-

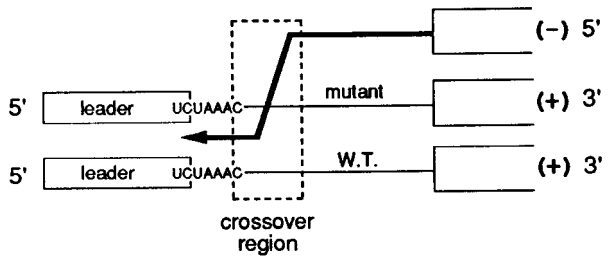

FIG. 7. Model for leader recombination during minus-strand synthesis. The model shows the alignment of two positive-strand templates, one the mutant and the other the wild type (W.T.), and indicates a polymerase switching from one template (donor) to the other (acceptor) during minus-strand synthesis. The leader is indicated by the smaller open rectangle, and the region of the genomic 5′-proximal open reading frame is indicated by the larger open rectangle. The most probable polymerase crossover region as determined in this study is indicated by a window drawn with a dashed line.

fected cells at early times postinfection that is not an integral part of mRNA or genomic molecules.

DISCUSSION

We have shown in experiments presented here that the 5′-proximal DI genomic leader-flanking UCUAAAC promoter motif is not required on the positive-strand input DI RNA for recombination-mediated conversion of an extensively mutated leader in the transfected DI RNA. Thus, leader conversion could not have happened through a leader priming of replication using an AGAUUUG promoter on the minus-strand copy of input DI RNA. Another mechanism must therefore explain leader conversion. Furthermore, although structure probing analysis of the BCV 5′ terminus (nt 1 through 130) indicates that the singular UCUAAAC sequence element is in the loop of a prominent stem-loop (Fig. 1C) and is thus theoretically accessible for base-paired RNA-RNA interactions (8) of the kind originally postulated for leader priming of transcription (2, 4, 21, 31, 32), evidence of a free leader at early times postinfection was lacking in an RNase protection assay (Fig. 6). Taken together, these results would not lend direct support to a common mechanism of leader-primed transcription for explaining leader conversion in BCV-infected cells.

What alternative mechanism could explain leader recombination (conversion) as observed here? One explanation might be a modified leader-priming model in which a free leader, perhaps one occurring later than 3 hpi, uses a sequence other than the 5′-proximal leader-flanking UCUAAAC element for leader priming of replication. Makino and Lai (30) and Jeong and Makino (16), for example, have suggested that some portion of the 9-nt UUUAUAAAC sequence occurring just downstream of the leader-associated UCUAAAC element, a region shown to be a hot spot for leader recombination in MHV (16, 26, 30), might function in the priming event for the generation of DI RNAs lacking the 9-nt sequence. A priming event using this sequence, however, cannot be a requirement for DI RNA replication since many naturally occurring MHV DI RNAs lacking the 9-nt sequence still replicate (16, 30). Thus, a priming site for DI RNA replication, were priming to happen, remains to be determined. We suggest an alternative mechanism for leader recombination that does not employ the use of a free leader. A preponderance of evidence supports the notion that both homologous and nonhomologous recombination among RNA viruses results from a polymerase strand switching (copy choice) during either plus- or minus-strand synthesis rather than by a chain breakage and religation (14, 15, 18, 22, 41). A possible mechanism for leader recombination, therefore, is one in which polymerase strand switching occurs during minus-strand synthesis (Fig. 7). This idea is suggested first by the data showing the recombination crossover region to be virtually all downstream of the leader-flanking UCUAAAC sequence and thus downstream of the leader, a pattern that would fit a process of strand switching during minus-strand synthesis (14). Furthermore, since many extensively mutated leaders were repaired similarly (both in reference 7 and in this study), it would seem that a region downstream of the UCUAAAC motif directs the recognition step in the leader recombination event. This notion is supported by the results of an extensive deletion in the downstream palindromic UUUAUAAA sequence which prevented recombination and replication (pDrepM3; Fig. 3) and by a similar natural deletion in MHV DI RNA that correlated with no leader recombination (30). Curiously, the 5′ terminus of the BCV leader is also an important region for recombination (7). This could possibly reflect a requirement of the 5′ terminus for leader alignment before recombination, for minus-strand synthesis of the DI RNA molecule, or for some other unknown function. Second, this mechanism has the attraction that leader-containing plus-strand (genomic and mRNA) molecules are abundant during virus replication, a plus-to-minus ratio of at least 10:1 for BCV (12), and provide a ready template for strand switching and synthesis of wild-type antileader on the 3′ terminus of the DI RNA minus strand. It has been argued in the case of poliovirus recombination, which is documented to occur during minus-strand synthesis (19), that the rate-limiting step in recombination is reassociation of the polymerase with the acceptor template (14, 15). Since reassociation is a second-order reaction, its rate will be strongly influenced by the concentration of the acceptor molecule (15). Similar circumstances support the notion of recombination during minus-strand synthesis in flock house virus (25). Polymerase switching during minus-strand synthesis has also been put forth as one of several possible mechanisms to explain the results of experiments in which transfected synthetic 5′ UTR sequences directed leader conversion on MHV genomic RNA in MHV-infected cells (26). One notable difference between the leader conversion reported here for BCV DI RNA and the leader conversion in MHV genomic RNA (26), however, is that crossovers did not occur downstream of base 94 in BCV DI RNA even after four virus passages, whereas in MHV genomic RNA they occurred throughout the 5′ UTR and even within the polymerase open reading frame. Further studies are needed to determine whether the recombination described for MHV with synthetic molecules (26) and that described here for BCV with DI RNA have a common mechanism.

Does leader conversion on DI RNA result from the same mechanism giving rise to leader fusion during subgenomic transcription? Assuming the basic scheme for leader fusion is as described in the legend to Fig. 7 for both processes, an immediately obvious difference between the two processes would be the degree of potential sequence identities that exists between the donor and acceptor templates. In DI RNA replication, the entire 498-nt DI RNA 5′ terminus has sequence identity with the virus genome 5′ terminus, creating a situation for homologous recombination, whereas during subgenomic transcription, only the UCUAAAC promoter motif and fortuitous flanking sequences (4) provide the identity, creating a situation more akin to nonhomologous recombination (15, 22, 41). Many mechanistic details of the two processes may, therefore, differ, and many extrapolations might not be possible. Perhaps, for example, the UCUAAAC promoter motif is critically important during subgenomic transcription (20, 27, 45)

but can be dispensed with during leader conversion on DI RNA (this study).

Some features, on the other hand, might be shared between the two processes. It has been proposed (35) that attenuated synthesis of minus-strand RNA at intergenic sites (possibly at the UCUAAAC elements) is the mechanism by which subgenomic minus-strand molecules, postulated templates for transcription of subgenomic mRNAs (3, 9, 12, 35–38), are generated. In the proposal, it was suggested that leader fusion might arise from a leader-priming event using a leader supplied in *trans*, or possibly from splicing of the plus- or minus-strand genomic RNA to provide a leader-containing template (35). We suggest here and elsewhere (20) that strand switching during minus-strand synthesis to provide an antileader on subgenomic minus strands (37) might be a fundamental process shared with that of leader conversion on DI RNA, although the crossover sites would not necessarily be the same. This idea has the attraction that the plus-strand leader templates, presumably on mRNAs, in addition to being abundant and thus favoring the second-order reaction described above, would not be destroyed. Thus, an abundant renewable source of free leader would not be required in this model for subgenomic mRNA synthesis, nor would there be a requirement for polymerase trimming of a large free leader 3′ terminus to adjust its size to that of the fused leader on mRNA (1, 21, 45). Furthermore, the crossover activity of the enzyme could be processive (15) as postulated to be the case during coronavirus intragenic recombination (28) and poliovirus recombination (14).

Is the structure of the BCV leader one that would suggest accessibility as a template for polymerase strand switching? Mechanisms directing strand switching by RNA-dependent RNA polymerases are in general poorly understood and may, in fact, not be the same for all RNA viruses (14, 15, 21, 41). In some cases, including intragenic recombination in coronaviruses (28) and polioviruses (19) and intergenic crossover in brome mosaic virus (41), regions of homology, or possibly even complementarity, appear important for inducing the crossover event. In other cases, including nonhomologous recombination between virus-associated satellite RNA, DI RNA, and genomic RNAs of turnip crinkle virus (5), regions of secondary structure appear critical in determining crossover sites. Although stem II and its loop containing the UCUAAAC sequence were demonstrably unimportant in the rapid site-specific recombination observed here for leader conversion on DI RNA, they might be important for polymerase strand switching during subgenomic mRNA synthesis. Certainly the stem-loop structure would seem to place the UCUAAAC motif in a position of availability for RNA-RNA base pairing (8), and thus it may play a role in polymerase strand switching during minus-strand synthesis. A relatively stable stem-loop, stem-loop III, is predicted by the Tinoco algorithm (44) to occur 18 nt downstream of the UUUAUAAA palindromic sequence for BCV (−7.2 kcal/mol) (Fig. 1C), 17 nt downstream for MHV (−10.2 kcal/mol), and 7 nt downstream for TGEV (−5.2 kcal/mol). This structure might contribute to a polymerase pause during minus-strand synthesis and thus contribute to template switching. Its role requires further investigation. Likewise, structure probing of the leader and flanking UTR sequences of other coronaviruses is needed to identify potentially phylogenetically conserved domains that might also suggest a mechanism for strand switching.

ACKNOWLEDGMENTS

We thank David Hacker, Paul Masters, and Stanley Sawicki for helpful discussions of the manuscript.

This work was supported mostly by grant 92-37204-8046 from the U.S. Department of Agriculture and partly by grant AI 14367 from the National Institutes of Health and funds from the University of Tennessee, College of Veterinary Medicine, Center of Excellence Program for Livestock Diseases and Human Health.

REFERENCES

1. **Baker, S. C., and M. M. C. Lai.** 1990. An in vitro system for the leader-primed transcription of coronavirus mRNAs. EMBO J. **9:**4173–4179.
2. **Baric, R. S., C.-K. Shieh, S. A. Stohlman, and M. M. C. Lai.** 1987. Analysis of intracellular small RNAs of mouse hepatitis virus: evidence for discontinuous transcription. Virology **156:**342–354.
3. **Brian, D. A., R.-Y. Chang, P. B. Sethna, and M. A. Hofmann.** 1993. Role of subgenomic minus-strand RNA in coronavirus replication. Arch. Virol. Suppl. **9:**173–180.
4. **Budzilowicz, C. J., S. Wikzynski, and S. R. Weiss.** 1985. Three intergenic regions of nucleotide sequence that are homologous to the 3′ end of the viral mRNA leader sequence. J. Virol. **53:**834–840.
5. **Carpenter, C. D., J.-W. Oh, C. Zhang, and A. E. Simon.** 1995. Involvement of a stem-loop structure in the location of junction sites in viral RNA recombination. J. Mol. Biol. **245:**608–622.
6. **Chang, R.-Y., and D. A. Brian.** 1996. *cis* requirement of N-specific protein sequence in bovine coronavirus defective interfering RNA replication. J. Virol. **70:**2201–2207.
7. **Chang, R.-Y., M. A. Hofmann, P. B. Sethna, and D. A. Brian.** 1994. A *cis*-acting function for the coronavirus leader in defective interfering RNA replication. J. Virol. **68:**8223–8231.
8. **Chastain, M., and I. Tinoco.** 1991. Structural elements in RNA. Prog. Nucleic Acid Res. Mol. Biol. **41:**131–177.
9. **Hofmann, M. A., and D. A. Brian.** 1991. The 5-prime end of coronavirus minus-strand RNAs contain a short poly(U) tract. J. Virol. **65:**6331–6333.
10. **Hofmann, M. A., R.-Y. Chang, S. Ku, and D. A. Brian.** 1993. Leader-mRNA junction sequences are unique for each subgenomic mRNA species in the bovine coronavirus and remains so throughout persistent infection. Virology **196:**163–171.
11. **Hofmann, M. A., S. D. Senanayake, and D. A. Brian.** 1993. A translation-attenuating intraleader open reading frame is selected on coronavirus mRNAs during persistent infection. Proc. Natl. Acad. Sci. USA **90:**11733–11737.
12. **Hofmann, M. A., P. B. Sethna, and D. A. Brian.** 1990. Bovine coronavirus mRNA replication continues throughout persistent infection in cell culture. J. Virol. **64:**4108–4114.
13. **Jaeger, J. A., D. H. Turner, and M. Zuker.** 1989. Improved predictions of secondary structure of RNA. Proc. Natl. Acad. Sci. USA **86:**7706–7710.
14. **Jarvis, T. C., and K. Kirkegaard.** 1991. The polymerase in its labyrinth: mechanisms and implications of RNA recombination. Trends Genet. **7:**186–191.
15. **Jarvis, T. C., and K. Kirkegaard.** 1992. Poliovirus RNA recombination: mechanistic studies in the absence of selection. EMBO J. **11:**3135–3145.
16. **Jeong, Y. S., and S. Makino.** 1994. Evidence for coronavirus discontinuous transcription. J. Virol. **68:**2615–2623.
17. **Joo, M., and S. Makino.** 1992. Mutagenic analysis of the coronavirus intergenic consensus sequence. J. Virol. **66:**6330–6337.
18. **King, A. M. Q.** 1988. Genetic recombination in positive strand RNA viruses, p. 149–165. *In* E. Domingo, J. J. Holland, and P. Ahlquist (ed.), RNA genetics, vol. II. CRC Press, Inc., Boca Raton, Fla.
19. **Kirkegaard, K., and D. Baltimore.** 1986. The mechanism of RNA recombination in poliovirus. Cell **47:**433–443.
20. **Krishnan, R., R.-Y. Chang, and D. A. Brian.** Tandem placement of a coronavirus promoter results in enhanced mRNA synthesis from the downstream-most initiation site. Virology, in press.
21. **Lai, M. M. C.** 1990. Coronavirus: organization, replication, and expression of genome. Annu. Rev. Microbiol. **44:**303–333.
22. **Lai, M. M. C.** 1992. RNA recombination in animal and plant viruses. Microbiol. Rev. **56:**61–79.
23. **La Monica, N., K. Yokomori, and M. M. C. Lai.** 1992. Coronavirus mRNA synthesis: identification of novel transcription initiation signals which are differentially regulated by different leader sequences. Virology **188:**402–407.
24. **Lapps, W., B. G. Hogue, and D. A. Brian.** 1987. Sequence analysis of the bovine coronavirus nucleocapsid and matrix protein genes. Virology **157:**47–57.
25. **Li, Y., and L. A. Ball.** 1993. Nonhomologous RNA recombination during negative-strand synthesis of flock house virus RNA. J. Virol. **67:**3854–3860.
26. **Liao, C.-L., and M. M. C. Lai.** 1992. RNA recombination in a coronavirus: recombination between viral genomic RNA and transfected RNA fragments. J. Virol. **66:**6117–6124.
27. **Makino, S., and M. Joo.** 1993. Effect of intergenic consensus flanking sequences on coronavirus transcription. J. Virol. **67:**3304–3311.
28. **Makino, S., J. G. Keck, S. A. Stohlman, and M. M. C. Lai.** 1986. High-frequency recombination of murine coronaviruses. J. Virol. **57:**729–737.
29. **Makino, S., and M. M. C. Lai.** 1989. Evolution of the 5′-end of genomic RNA of murine coronaviruses during passages in vitro. Virology **169:**227–232.

30. **Makino, S., and M. M. C. Lai.** 1989. High-frequency leader sequence switching during coronavirus defective interfering RNA replication. J. Virol. **63:** 5285–5292.
31. **Makino, S., L. H. Soe, C.-K. Shieh, and M. M. C. Lai.** 1988. Discontinuous transcription generates heterogeneity at the leader fusion sites of coronavirus mRNAs. J. Virol. **62:**3870–3873.
32. **Makino, S., S. Stohlman, and M. M. C. Lai.** 1986. Leader sequence of murine coronavirus mRNAs can be freely reassorted: evidence for the role of free leader RNA in transcription. Proc. Natl. Acad. Sci. USA **83:**4204–4208.
33. **Pollack, J. R., and D. Ganem.** 1993. An RNA stem-loop structure directs hepatitis B virus genomic RNA encapsidation. J. Virol. **67:**3254–3263.
34. **Sambrook, J., E. F. Fritsch, and T. Maniatis.** 1989. Molecular cloning: a laboratory manual, 2nd ed. Cold Spring Harbor Laboratory, Cold Spring Harbor, N.Y.
35. **Sawicki, S. G., and D. L. Sawicki.** 1990. Coronavirus transcription: subgenomic mouse hepatitis virus replicative intermediates function in mRNA synthesis. J. Virol. **64:**1050–1056.
36. **Schaad, M. C., and R. S. Baric.** 1994. Genetics of mouse hepatitis virus transcription: evidence that subgenomic negative strands are functional templates. J. Virol. **68:**8169–8179.
37. **Sethna, P. B., M. A. Hofmann, and D. A. Brian.** 1991. Minus-strand copies of replicating coronavirus mRNAs contain antileaders. J. Virol. **65:**320–325.
38. **Sethna, P. B., S.-L. Hung, and D. A. Brian.** 1989. Coronavirus subgenomic minus-strand RNA and the potential for mRNA replicons. Proc. Natl. Acad. Sci. USA **86:**5626–5630.
39. **Shieh, C.-K., H.-J. Lee, K. Yokomori, N. La Monica, and M. M. C. Lai.** 1989. Identification of a new transcriptional initiation site and the corresponding functional gene 2b in the murine coronavirus RNA genome. J. Virol. **63:** 3729–3736.
40. **Shieh, C.-K., L. H. Soe, S. Makino, M.-F. Chang, S. A. Stohlman, and M. M. C. Lai.** 1987. The 5′-end sequence of the murine coronavirus genome: implications for multiple fusion sites in leader-primed transcription. Virology **156:**321–330.
41. **Simon, A. E., and J. J. Bujarski.** 1994. RNA-RNA recombination and evolution in virus-infected plants. Annu. Rev. Phytopathol. **32:**337–362.
42. **Skinner, M. A., V. R. Racaniello, G. Dunn, J. Cooper, P. D. Minor, and J. W. Almond.** 1989. New model for the secondary structure of the 5′ non-coding RNA of poliovirus is supported by biochemical and genetic data that also show that RNA secondary structure is important in neurovirulence. J. Mol. Biol. **207:**379–392.
43. **Spaan, W., H. Delius, M. Skinner, J. Armstrong, P. Rottier, S. Smeekens, B. A. van der Ziejst, and S. G. Siddell.** 1983. Coronavirus mRNA synthesis involves fusion of non-contiguous sequences. EMBO J. **2:**1839–1844.
44. **Tinoco, I., P. N. Borer, B. Dengler, M. D. Levine, O. C. Uhlenbeck, D. M. Crothers, and J. Gralla.** 1973. Improved estimation of secondary structure in ribonucleic acids. Nature (London) New Biol. **246:**40–41.
45. **Van der Most, R. G., R. J. DeGroot, and W. J. M. Spaan.** 1994. Subgenomic RNA synthesis directed by a synthetic defective interfering RNA of mouse hepatitis virus: a study of coronavirus transcription initiation. J. Virol. **68:** 3656–3666.
46. **Yokomori, K., L. R. Banner, and M. M. C. Lai.** 1991. Heterogeneity of gene expression of hemagglutinin-esterase (HE) protein of murine coronavirus. Virology **183:**647–657.
47. **Zhang, X., and M. M. C. Lai.** 1994. Unusual heterogeneity of leader-mRNA fusion in a murine coronavirus: implications for the mechanism of RNA transcription and recombination. J. Virol. **68:**6626–6633.